International Journal of Progressive Sciences and Technologies (IJPSAT)
ISSN: 2509-0119.

https://ijpsat.org/
Vol. 54 No. 1 December 2025, pp. 530-547

Contribution Of The Rusle Model To The Analysis Of Erosion Trends In The Mananasy- Tamponala Watershed: Soavinandriana District

HERITAHINA Rambeloson[1,2], RASOLOMANANA Eddy Harilala[1,3], RANDRIANJA Kanto Volahasina[1,2]

[1]Doctoral School Engineering and Geoscience, University of Antananarivo, Madagascar
[2] University of Itasy
[3]Polytechnic School of Antananarivo
Corresponding Author: HERITAHINA Rambeloson

Abstract— This study analyzes the spatio-temporal evolution of soil erosion in the Mananasy Tamponala watershed between 2016 and 2024. It is based on the RUSLE model coupled with remote sensing and GIS data. The R factor is derived from monthly precipitation, factor K is calculated from SoilGrids soil data, factor LS comes from a high-resolution DTM, factor C is estimated using NDVI images, and factor P integrates the land cover map via WorldCover and slope. The quantitative results show a median soil loss of approximately 57 t·ha⁻¹·year⁻¹ in 2022. Factor R increases from approximately 600 to 686 MJ·mm·ha⁻¹·h⁻¹ between 2016– 2020 and 2022, and factor C reaches 0.521 in 2022. At the same time, the proportion of land in extreme erosion classes (> 50 t·ha⁻¹·year⁻¹) increases from 4.72% in 2020 to 21.19% in 2022. These changes highlight the Itasy's high sensitivity to extreme precipitation and vegetation cover degradation, which requires integrated and sustainable soil management.
Keywords: RUSLE, Mananasy Tamponala, Watershed, Water erosion, Soil management

I. INTRODUCTION

Madagascar, and more particularly the Itasy region in the Highlands, is highly exposed to water erosion due to a combination of steep slopes, intense rainfall events, and increasing land pressure. This erosion manifests itself in particular through lavaka, which cut into the slopes, export the topsoil and contribute to the silting up of water bodies, including Lake Itasy. Work carried out in the Highlands has shown that geology, topography, and land use dynamics are major determinants of the distribution and intensity of these forms of erosion. [1]

Within this region, the Mananasy–Tamponala watershed, located in the district of Soavinandriana, is a particularly sensitive area where steep slopes, intensive farming, and sediment accumulation zones coexist. It extends over the rural communes of Mananasy (upstream) and Tamponala (downstream), which are characterized by intensive agricultural development, relative isolation, and heavy pressure on natural resources. These communes are rich in natural resources such as hot springs, lakes, gold, and precious stones, the exploitation of which sometimes generates uncontrolled land use dynamics. In addition, the presence of artisanal quarries that do not comply with technical extraction and stabilization standards contributes to the destructuring of slopes, weakens soils, and increases local susceptibility to erosion. Despite numerous local observations, there is still a lack of an integrated and diachronic understanding of erosion in this watershed that can pinpoint where and when soil loss is intensifying, identify areas that are critically vulnerable in the long term, and link these dynamics to the main controlling factors (rainfall, soil type, topography, land cover, anthropogenic practices and pressures [2][3].

International Journal of Progressive Sciences and Technologies (IJPSAT)
ISSN: 2509-0119.

https://ijpsat.org/
Vol. 54 No. 1 December 2025, pp. 530-547

To address this deficiency, this research adopts the RUSLE (Revised Universal Soil Loss Equation) model, which explicitly links five factors: rainfall erosivity, soil erodibility, slope length and gradient, crop cover and management, and anti-erosion practices to average annual soil loss [4].

The overall objective is to analyze the spatial and temporal evolution of soil erosion in the Mananasy-Tamponala watershed. More specifically, the specific objectives are to: parameterize the RUSLE factors for several periods; estimate and map soil losses on several reference dates. We then begin by hypothesizing that topographical conditions explain a large part of the erosion hotspots observed on the steep slopes of the Highlands. We then argue that the increase in cultivated areas with low cover increases the C factor and results in increased soil loss near agricultural areas. We also assume that anti-erosion practices (contour farming, grass strips, hedges) reduce the severity of losses. Finally, we consider that interannual rainfall variability modulates erosivity and contributes to temporal contrasts in erosion.

To better understand this, the work is divided into three main parts. The first part, titled Materials and Methods, provides a detailed description of the study area and the data used, including rainfall, satellite imagery, and topographic parameters. It also describes the analytical methods and tools used, such as erosion, spatio-temporal indices, and statistical and geospatial analyses. The second part presents the results obtained and analyzes the trends observed over time and space. The third part discusses the findings.

II. STUDY AREA

II.1. Presentation of the study area

The Itasy region is located in central Madagascar, approximately 120 kilometers west of Antananarivo. It covers an area of approximately 6,900 km² and comprises three main districts: Miarinarivo, Soavinandriana, and Arivonimamo. Its landscape is dominated by hills and plateaus of volcanic origin, dotted with numerous lakes and craters, including the famous Lake Itasy, which is the largest inland body of water in the country. In the district of Soavinandriana, the Mananasy–Tamponala watershed, which is our study area, lies within two rural municipalities: the municipality of Mananasy upstream and the municipality of Tamponala downstream. These municipalities are characterized by steep slopes, volcanic hill landscapes carved by a dense hydrographic network, and land use dominated by food crops, lowland rice fields, and pastures.[2] [5]

The hydrographic network is dense and mainly oriented towards the west, feeding numerous small watersheds, including that of Mananasy–Tamponala. The climate, which is tropical at altitude, is characterized by a marked rainy season (November to April) and a cooler dry season (May to October). Annual rainfall varies between 1,200 and 1,800 mm, promoting both agricultural productivity and the risk of water erosion on slopes. [4]

International Journal of Progressive Sciences and Technologies (IJPSAT)
ISSN: 2509-0119.

https://ijpsat.org/
Vol. 54 No. 1 December 2025, pp. 530-547

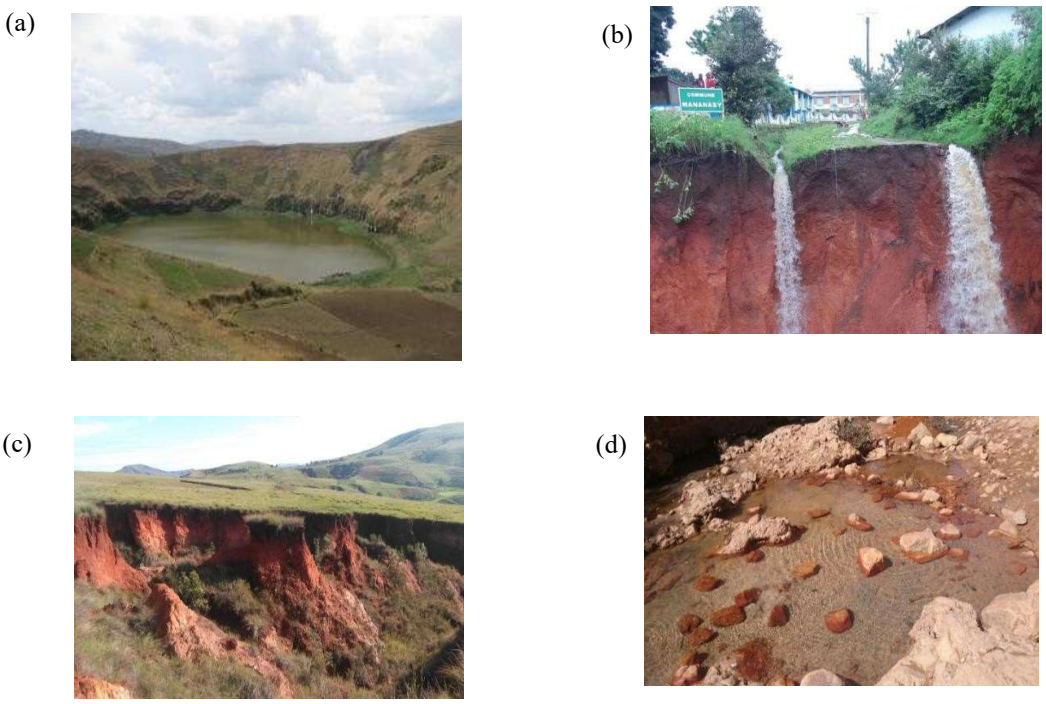

Figure1: (a) Lake Andranomaintso-Manansy, (b) unmaintained ravine (Andrinanatenanina M, 2017), (c) Tamponala lavaka phenomenon, (d) Mananasy hot springs

The soils are dominated locally by Andosols derived from recent volcanic materials characterized by low bulk density, high organic matter content, and amorphous products (allophane) intermingled with older ferralitic soils, which strongly influences the erodibility and water response of the slope. [6]

Land use and cropping systems combine rice cultivation (seasonal and off-season irrigated, and rainfed) in the valley bottoms, cereals (corn), roots and tubers (cassava, potatoes), legumes (beans), and market gardening. The economy in the Soavinandriana district is based mainly on agriculture, livestock farming, fishing, and tourism. Agricultural practices are largely traditional, using hand tools and few soil conservation techniques. [3][7] . Cattle and sheep farming is an important complementary activity, but overgrazing contributes to soil degradation and the depletion of grass cover. Craft activities (brickworks, charcoal production, local tanneries) and bush fires linked to pasture renewal increase pressure on natural resources. The expansion of often unplanned residential areas and the informal exploitation of construction materials exacerbate landscape fragmentation and slope destabilization. [8]

The map below shows the location of the Soavinandriana district.

International Journal of Progressive Sciences and Technologies (IJPSAT)
ISSN: 2509-0119.

https://ijpsat.org/
Vol. 54 No. 1 December 2025, pp. 530-547

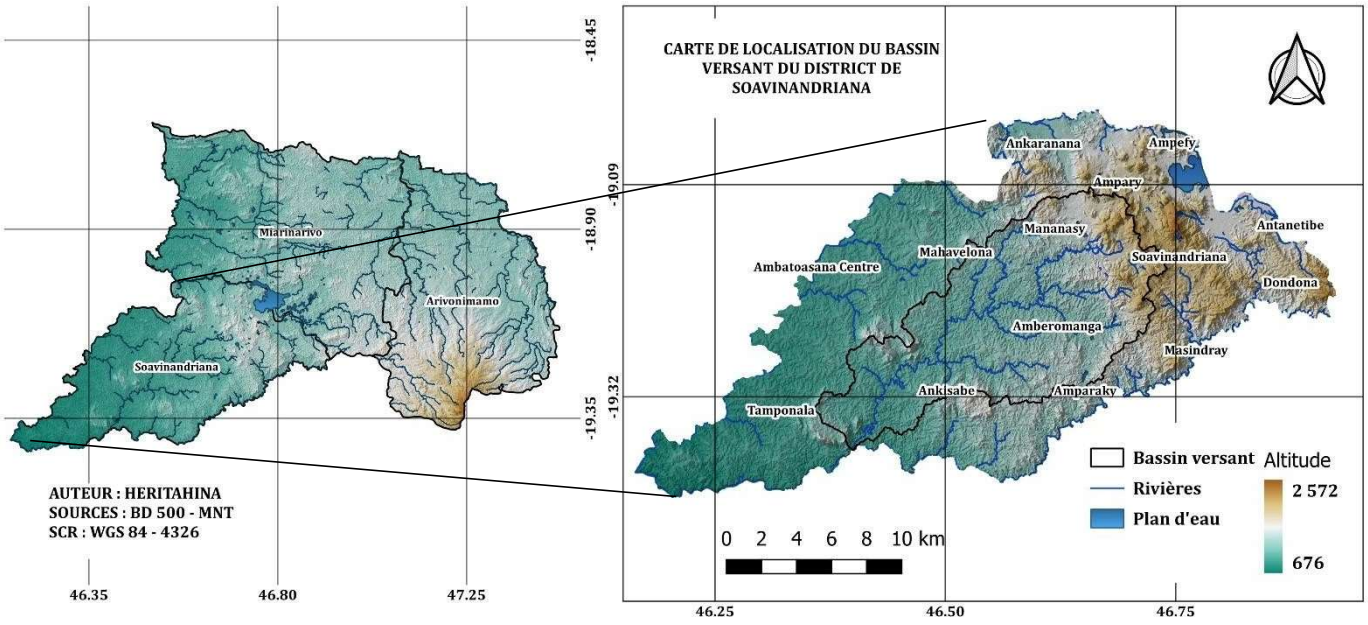

Map 1: location map of the Soavinandriana district watershed

III. DATA AND METHODS

This work is based primarily on meteorological, topographical, land use/land cover, soil, and satellite data. These datasets were used to assess soil erosion on a biannual basis, as well as erosion factors in the study area. Several geospatial data sources were used to carry out this study, based on a working environment combining remote sensing and Geographic Information System tools, which are shown in the following table (1):

Table1: Data inventory

Data	Sources	Resolution
Rainfall Data	Climate Hazards Group InfraRed Precipitation with Station data (CHIRPS)	/
Land Use / Land cover	ESA WorldCover 2020 (https://worldcover2020.esa.int/)	10m
NDVI (Normalized Difference Vegetation Index)	Normalized Difference Vegetation Index): Sentinel 2 Copernicus imagery, retrieved from Google Earth Engine for years 2016, 2018, 2020, 2022, and 2024.	20m
Digital Elevation Model (DEM)	NASA Earth Observation Data (https://www.earthdata.nasa.gov/data/instruments/srtm)	30 m
Soil and Land Use	SoilGrids and WoSIS (https://soilgrids.org/)	250m

III.1. Data processing flowchart for the RUSLE model

The following flowchart schematically shows the organization of data and factors in the soil loss equation (RUSLE) in order to illustrate the logical chain from data sources to the spatialized assessment of average annual soil loss.

International Journal of Progressive Sciences and Technologies (IJPSAT)
ISSN: 2509-0119.

https://ijpsat.org/
Vol. 54 No. 1 December 2025, pp. 530-547

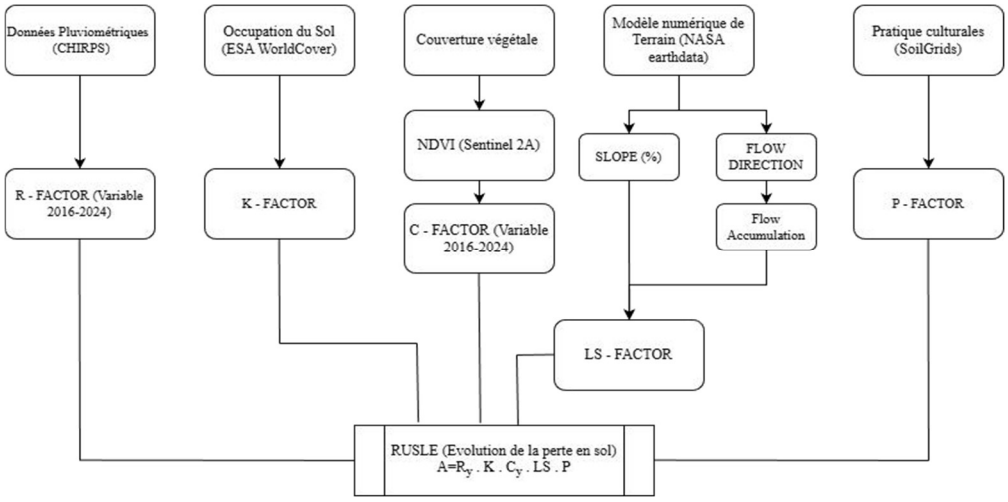

Figure 2: Flowchart of RUSLE model factors used to analyze soil loss potential in the Soavinandriana district watershed

III.2. Erosion estimation methodology

The quantitative estimation of soil erosion was carried out using the **RUSLE** (Revised Universal Soil Loss Equation) model, which calculates the average annual soil loss (A, in tons per hectare per year) as the product of five multiplicative factors [8]:

$$A = R \times K \times LS \times C \times P$$

Where:

A: Annual soil loss rate expressed in $t.ha^{-1}.an^{-1}$

R: Rainfall erosivity factor expressed in $MJ \cdot mm \cdot ha^{-1} \cdot h^{-1} \cdot an^{-1}$;

K: Soil erodibility factor expressed in $t \cdot h \cdot MJ^{-1} \cdot mm^{-1}$;

LS: Topography factor (slope length and inclination);

C: Vegetation cover factor;

P: Anti-erosion farming practices factor

III.2.1. Rainfall erosivity factor (R)

In this study, the rainfall erosivity factor (R) was calculated from derivatives of monthly precipitation series from the CHIRPS satellite rainfall dataset for the period 2016- 2024, which provides near-global rainfall totals at 0.05° spatial resolution. [10]

For each year, the twelve-monthly totals were first calculated to obtain the annual precipitation; and then calculated using the following formula:

$$P_i = \sum_{m=1}^{12} P_m$$

International Journal of Progressive Sciences and Technologies (IJPSAT)
ISSN: 2509-0119.

https://ijpsat.org/
Vol. 54 No. 1 December 2025, pp. 530-547

Based on this average annual precipitation, the rainfall erosivity factor (R) was then estimated by applying the empirical relationship proposed by Lo and al. (1985), which linearly relates annual rainfall to the erosivity index in humid tropical conditions.[11] This equation is written as:

$$R = (38{,}46 + (3{,}48.\, P_i)\,.\,0{,}1$$

Where:

R: Rainfall erosivity factor expressed in $MJ \cdot mm \cdot ha^{-1} \cdot h^{-1} \cdot an^{-1}$

P_i : Annual precipitation expressed in $mm\,.\,an^{-1}$

III.2.2. Soil erodibility factor (K)

The soil erodibility factor (K) measures the intrinsic sensitivity of the soil to detachment and transport by the impact of raindrops and runoff. In our case, we calculate it using a standard empirical formula, the Wischmeier & Smith formula, in the parametric form proposed by Sharpley & Williams (1990). [12][13] This formula estimates K by combining the sand, silt, and clay content, organic carbon content, and soil structure/infiltration factors.

The Erosion/Productivity Impact Calculator (EPIC) equation is written as:

$$\mathrm{K} = \left\{0{,}2 + 0{,}3\exp\left[-0{,}0256\,SAN\left(1 - \frac{\mathrm{SAN}}{100}\right)\right]\right\}.\left(\frac{SIL}{CLA + SIL}\right)^{0{,}3}.\left(1 - \frac{0{,}25\,C}{C + \exp(3{,}72 - 2{,}95\,C)}\right).\left(1 - \frac{0.7\,SN1}{SN1 + \exp(-5.51 + 22.9\,SN1)}\right)$$

Where:

SAN = sand (% of particles 0.1–2 mm)

SIL = silt (% of particles 0.002–0.1 mm)

CLA = clay (% of particles < 0.002 mm)

C = organic carbon (%)

SN1 = $-SAN/100$

The coefficient 0.1317 is used to convert to the RUSLE unit, and the K obtained is c

III.2.3.Topography factor (LS)

LS is the topography factor combining slope length (L) and slope (S). It reflects the amplifying effect of relief on erosion: the longer and steeper the slope, the faster the runoff and the more soil is detached. In this study, the topography factor was calculated using the approach developed by Jim Pelton et al. in 2012, which expresses LS as a function of specific drainage area and slope, in order to better represent runoff convergence in a high-resolution DTM (10 m). [13] [14] LS was thus obtained using the following relationship

$$LS = (m + 1)\left[\frac{A}{22.1}\right]^{m}.\left[\frac{sin(\beta)}{0.09}\right]^{n}$$

The parameters m and n are constants whose values vary as follows: m=0.2 to 0.6 and n=1 to 1.3. Low values are used when sheet erosion is dominant, and maximum values are used when rill erosion is dominant. Due to the lack of detailed

International Journal of Progressive Sciences and Technologies (IJPSAT)
ISSN: 2509-0119.

https://ijpsat.org/
Vol. 54 No. 1 December 2025, pp. 530-547

information on the dominant form of erosion, the values m=0.4 and n=1.3 were adopted. This formula is translated into a GIS using the following formula:

$$LS = \left[\left(AccFlux.\frac{Dim_{pixel}}{22.1}\right)^{0.5}.(\sin\left(Pente_{deg}.\frac{3,14}{180}\right)/0.09)^{1.3}\right].1.3$$

Where:

$AccFlux$: flow accumulation map;

Dim_{pixel} dimension of the pixels on the flow accumulation map;

$Pente_{deg}$: slope map expressed in degrees;

(3.14/180): conversion factor from degrees to radians.

III.2.4. Vegetation cover factor (C)

The vegetation cover factor (C) is a dimensionless coefficient that reflects the ability of vegetation and cultivation practices to reduce soil loss compared to a bare, tilled control surface (C = 1). It depends mainly on the density and height of the cover, the coverage index, the proportion of herbaceous cover, and the presence of residues or litter on the soil surface. In the RUSLE literature, its values generally range from about 0.001 for very dense cover (forest, perennial crops) to 1 for bare or fallow soils. In order to spatialize this factor using remote sensing, we chose to use the method developed by Van der Knijff et al. (2000) [16], which consists of obtaining the C factor directly from the NDVI via a decreasing exponential function:

$$C_i = \begin{cases} 1, & if\ NDVI_i \leq 0 \\ e\left(-\alpha\frac{NDVI_i}{\beta - NDVI_i}\right), & if\ NDVI_i > 0 \end{cases}$$

where, α and β are parameters governing the shape of the NDVI–C curve. Following the recommendations of Van der Knijff et al. (2000), we took α =2, and β=1, values that allow for a realistic decrease in the C factor as surface vegetation density increases.

III.2.5. Cultivation practices factor (P)

The P factor was used to take into account anti-erosion practices, defined as the ratio between soil loss under the practice in question and that observed in the absence of the practice (plowing in the direction of the slope), in accordance with the definition of Renard et al. (1997) and the USDA Agriculture Handbook 703. P values were assigned based on slope and type of land use: P = 1 for no practice, 0.6–0.5 for crops grown on contour lines on gentle slopes, 0.3–0.6 for strip cropping, and ≤ 0.3 for terraced or bench-type land use. [17] The following table shows the main standard P values:

Table 2: Usual values for the P factor

Situation	Indicative P Value
No practice / plowing in the direction of the slope	1
Contour farming on gentle slope (≤ 2%)	0.6 – 0.7
Contour farming on 3–7% slope	0.5 – 0.6
Strip cropping	0.3 – 0.6 depending on strip width and slope
Bunds / terraces with closed outlets	0.1 – 0.3
Hedges/grass strips along contour lines	0.2 – 0.5
Terraced rice fields / full terracing	≤ 0.1

International Journal of Progressive Sciences and Technologies (IJPSAT)
ISSN: 2509-0119.

https://ijpsat.org/
Vol. 54 No. 1 December 2025, pp. 530-547

We derived the P factor, representing the effect of anti-erosion practices, from the ESA WorldCover land cover map, assigning appropriate P values to certain major land cover classes (forests, rainfed crops, terraced rice fields, bare land, etc.), based on the assumed degree of slope protection or development. The following figure shows the land cover map for the watershed

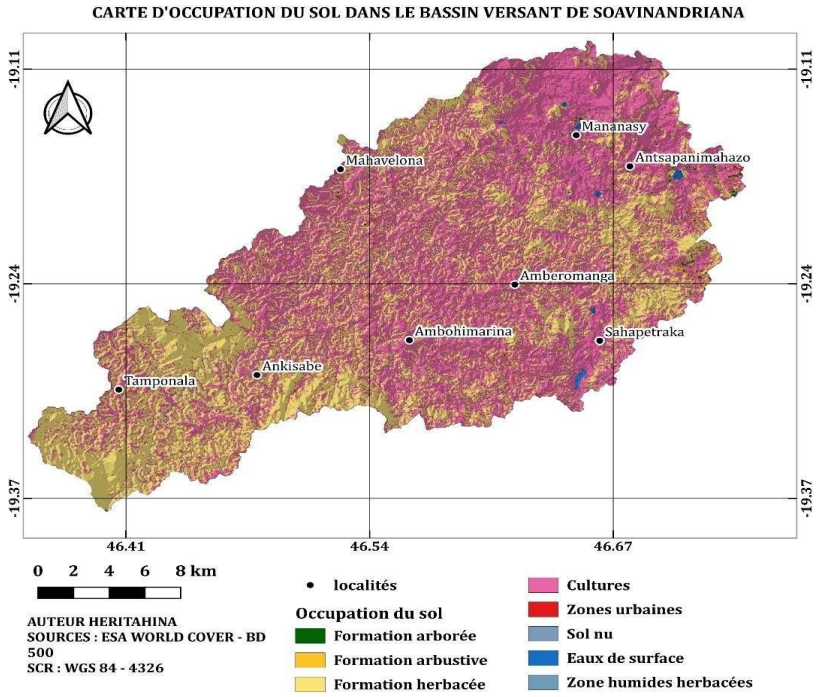

Map 2 : Land cover map of the Soavinandriana watershed

The land use map of the Soavinandriana watershed shows a clear predominance of crops (in pink), which cover most of the area, including around the main towns (Mananasy, Mahavelona, Amberomanga, Ambohimarina, Sahapetraka, Ankisabe, and Tamponala). Natural vegetation (trees, shrubs, and grasses) appears in scattered patches, mainly on slopes and in more rugged areas, reflecting a heavily anthropized landscape. Bare soil (gray-blue) and a few herbaceous wetlands are concentrated in certain low-lying areas and locally degraded sectors. Surface water (in blue) is limited in extent and appears in the form of small, scattered bodies of water.

IV. Results And Interpretations

IV.1. Modeling of Erosion Factors

IV.1.1. R Factor

The rainfall erosivity factor R was initially obtained from monthly precipitation data from the CHIRPS (Climate Hazards Group InfraRed Precipitation with Stations) satellite dataset, which provides near-global rainfall totals at 0.05° resolution since 1981. The annual series were then reconstructed by summing the 12 monthly values for each year. The average annual precipitation thus obtained over the study period was then entered into the empirical relationship proposed by Lo et al., which establishes a direct link between annual rainfall and the R factor, to estimate the average annual erosivity.

To describe the temporal evolution of rainfall erosivity for the entire period 2016– 2024, the R values were finally aggregated in two-year increments, using 2016, 2018, 2020, 2022, and 2024 as reference years. In addition to this rainfall reading, the erosivity factor R was estimated using the empirical relationship of Lo and al. generalized as follows:

International Journal of Progressive Sciences and Technologies (IJPSAT)
ISSN: 2509-0119.

https://ijpsat.org/
Vol. 54 No. 1 December 2025, pp. 530-547

$$\begin{cases} soit\ y\ \in \{2016,2018,2020,2022,2024\} \\ R_y = 0{,}1 \times \left(38{,}46 + 41.76P_y\right) \times 0{,}1 \end{cases}$$

The following map illustrates the variation in the R factor by two-year intervals between 2016 and 2024:

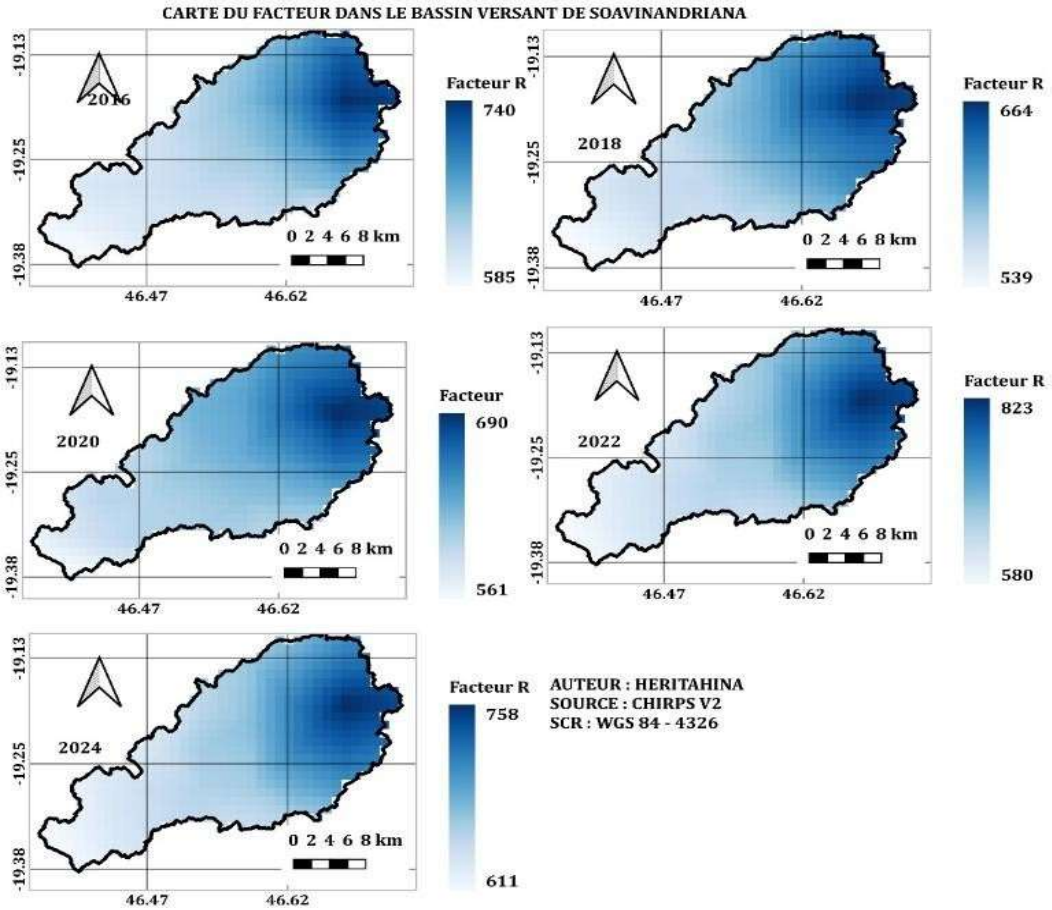

Map 3: Spatial distribution of the R factor in the Soavinandriana watershed

Over the entire study period, the R factor shows a marked spatial gradient, with values consistently higher in the northeast of the watershed and lower towards the southwest, indicating greater rainfall erosivity in the eastern upstream area. In terms of time, the average values of R vary from 600.7 to 686.3 MJ·mm·ha^{-1}·h^{-1}·year^{-1}, with a minimum in 2018, an increase in 2020, then a maximum in 2022, followed by values that remain high in 2024 (677.9). This fluctuation of around 15% between the least erosive and most erosive years reflects significant interannual variability in erosive rainfall, which tends to increase erosion

International Journal of Progressive Sciences and Technologies (IJPSAT)
ISSN: 2509-0119.

https://ijpsat.org/
Vol. 54 No. 1 December 2025, pp. 530-547

potential in recent years, particularly in the northeast of the basin. These values are represented by the histogram of the variation in the R factor over time in figure (3) below.

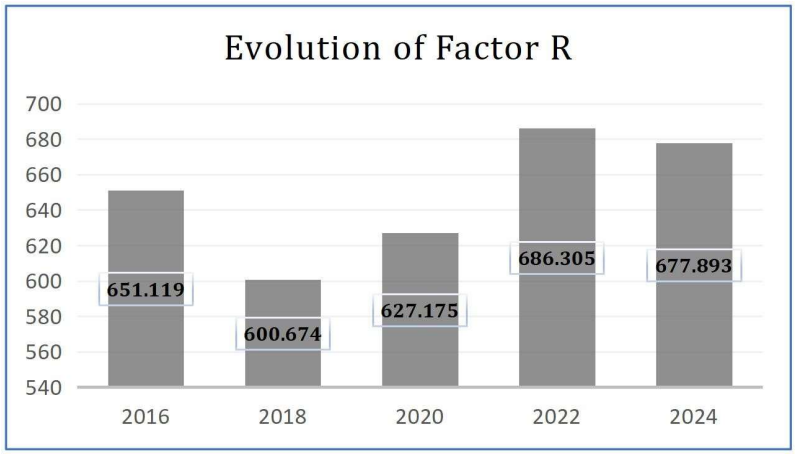

Figure 3: Histogram of variation in the R factor over time

IV.1.2. K factor

The K factor values from SoilGrids data range from 0.162 to 0.198 t·ha·h·(ha·MJ·mm)$^{-1}$, with an average of 0.1816 and a fairly low standard deviation (0.0052), indicating uniform soil erodibility across the entire watershed. These values are illustrated in the histogram in Figure 4.

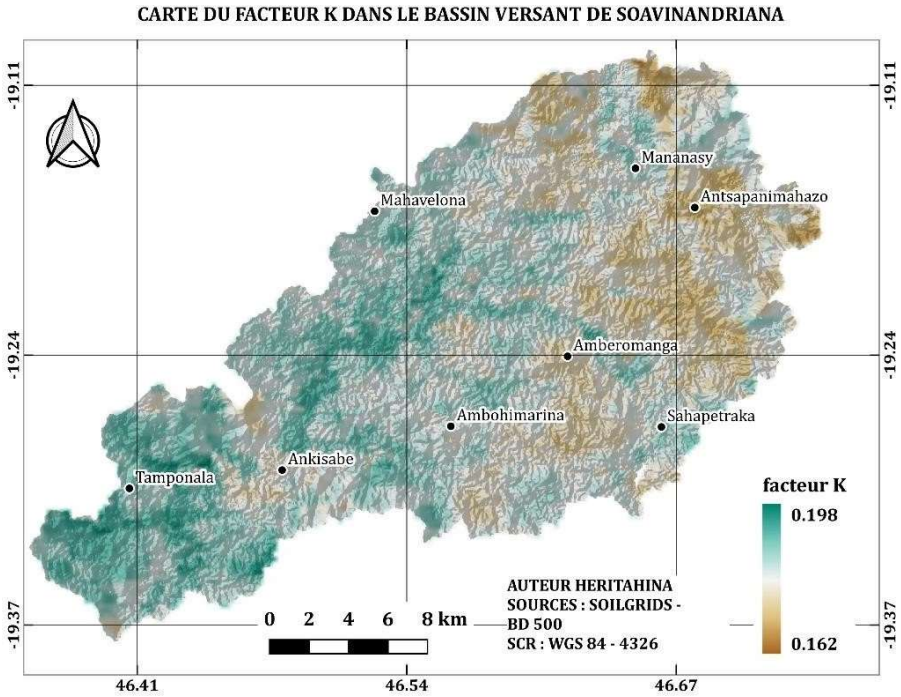

Map 4: K factor in the Soavinandriana watershed

International Journal of Progressive Sciences and Technologies (IJPSAT)
ISSN: 2509-0119.

https://ijpsat.org/
Vol. 54 No. 1 December 2025, pp. 530-547

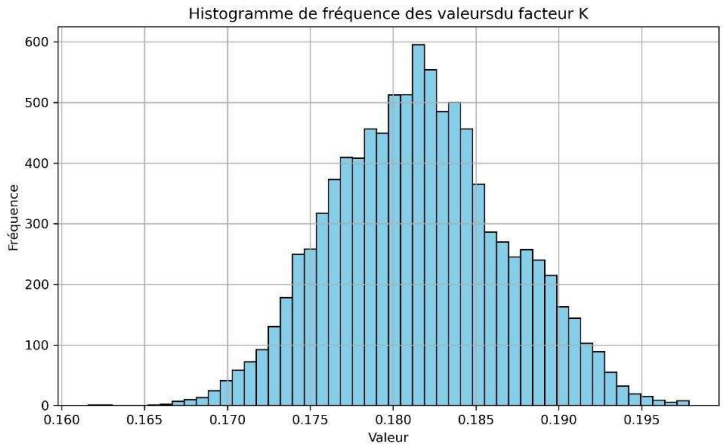

Figure 4 : Frequency histogram of K factor values

The histogram shows a near-normal distribution of values around 0.18, with the majority of pixels within a narrow range around this mean. The low standard deviation indicates that soil erodibility is generally moderate, with no areas of significant contrast in terms of intrinsic erodibility. Thus, for the region as observed in the watershed, spatial variations in erosion depend mainly on other RUSLE factors (slope/slope length, land use, conservation practices).

IV.1.3.LS factor

The LS topographic factor was calculated using the approach of Jim Pelton et al. (2012) for the Soavinandrina watershed and summarizes the combined effect of slope length and slope on erosion potential. Figure (4) shows that high LS values in red are mainly concentrated on the steepest slopes, often at the edge of thalwegs and along slope breaks, both in the upstream part (Mahavelona, Mananasy, and Antsapanimahazo) and in the more enclosed compartments to the southwest towards Tamponala. Conversely, low values (in blue-green) dominate the relatively flat interfluves, gently sloping lower slopes, and widened valley floor areas, reflecting a lower topographic contribution to potential erosion on these surfaces.

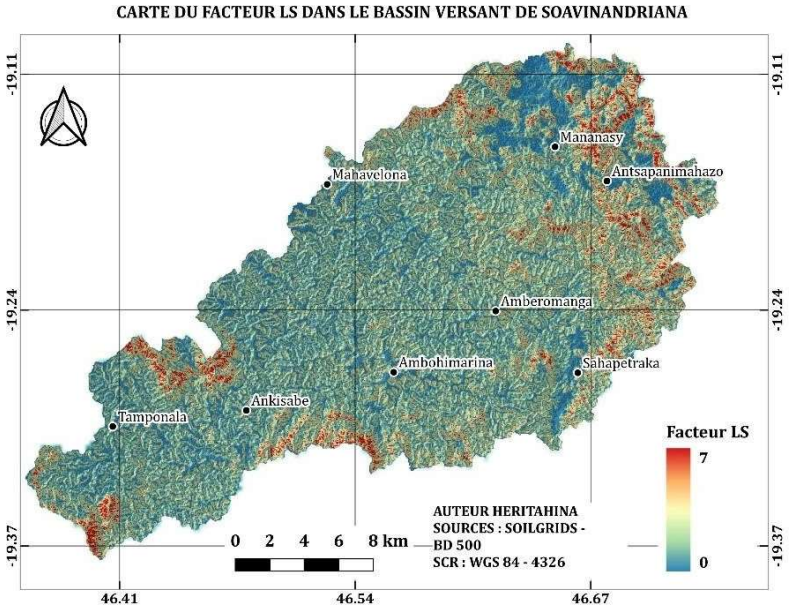

Map 5: LS factor in the Soavinandriana watershed

International Journal of Progressive Sciences and Technologies (IJPSAT)
ISSN: 2509-0119.

https://ijpsat.org/
Vol. 54 No. 1 December 2025, pp. 530-547

The interpretation of the LS is confirmed by the histogram, which shows a highly asymmetrical distribution, with a very large majority of pixels with a value <1, followed by numbers that decrease gradually as the LS increases, up to maximum values >6, which remain very much in the minority. This observation is nevertheless significant because it indicates that most of the basin is subject to moderate topographic control of erosion, while a relatively small proportion of the surface area is associated with either steep slopes or long runoff ramps.

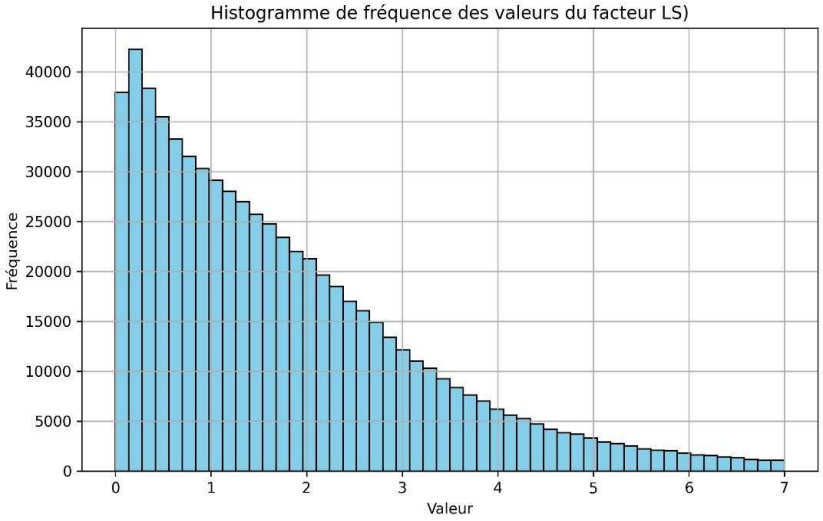

Figure 5: Frequency histogram of LS factor values

IV.1.4 C factor

Factor C was derived from NDVI images based on the method of Van der Knijff et al., namely an exponential relationship linking NDVI and factor C, thus allowing direct conversion from the vegetation cover density of a well-protected surface to highly

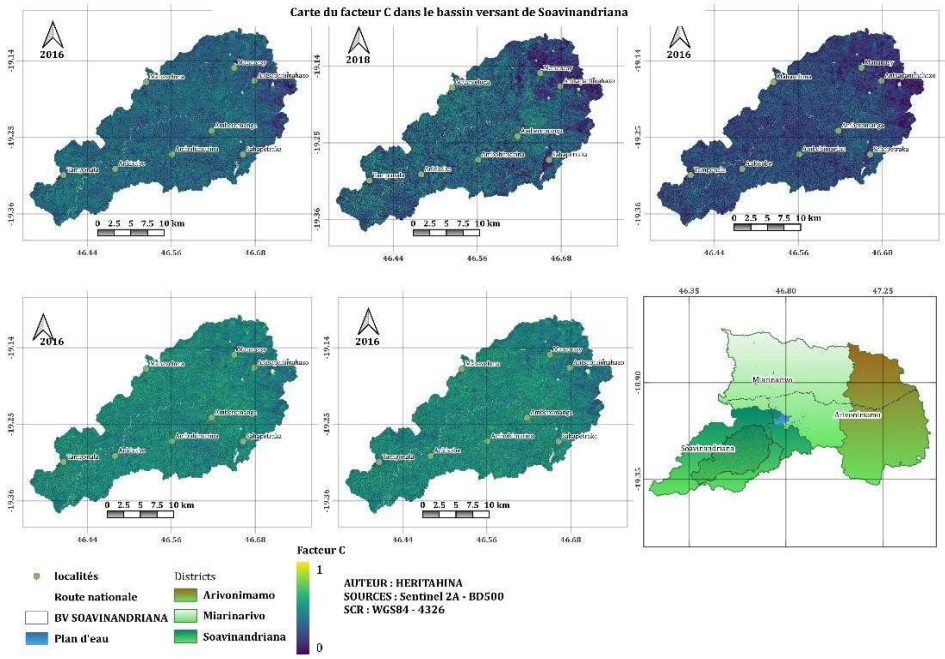

International Journal of Progressive Sciences and Technologies (IJPSAT)
ISSN: 2509-0119.

https://ijpsat.org/
Vol. 54 No. 1 December 2025, pp. 530-547

vulnerable bare soil. The figure below shows the spatial distribution of factor C in the Soavinandriana watershed for several years (2016, 2018, 2020, 2022, and 2024).

Map 6: Spatial distribution and distribution of Factor C in the Soavinandriana watershed

Spatially, the maps show a mosaic of generally low to intermediate values, with areas of low C corresponding to well-covered surfaces: flooded rice fields or dense vegetation, fragments of natural formations that are still closed. Conversely, higher C values appear around the main villages and along cultivated slopes, where annual crops dominate and the soil is partially bare. These areas reflect less protection of the soil against the impact of raindrops and an increased risk of particle detachment.

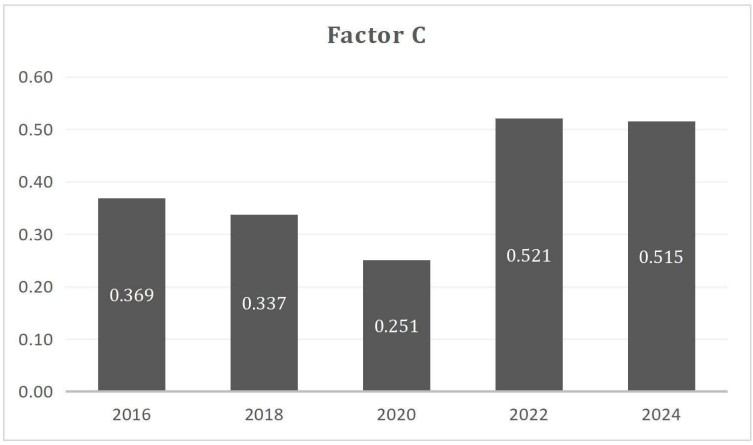

Figure 6: Evolution of Factor C over time

In the Soavinandriana watershed, Factor C remains moderate overall but changes significantly between 2016 and 2024. The average value will fall from 0.369 in 2016 to 0.337 in 2018, then drop to 0.251 in 2020, reflecting improved soil protection (more vegetation, less bare soil). From 2022 onwards, the trend reverses: the average C rises sharply to 0.521 in 2022, then remains high at 0.515 in 2024. In other words, the C factor for 2022–2024 is just over double that of 2020, indicating a significant deterioration in protective cover and therefore an increased risk of soil erosion in the recent period.

IV.1.5.P factor

To produce the P factor map for the watershed, we cross-referenced the ESA WorldCover 2020 land cover map with the USGS SRTM to spatialize the soil conservation practices included in the erosion model. The following figure illustrates the P factor map.

International Journal of Progressive Sciences and Technologies (IJPSAT)
ISSN: 2509-0119.

https://ijpsat.org/
Vol. 54 No. 1 December 2025, pp. 530-547

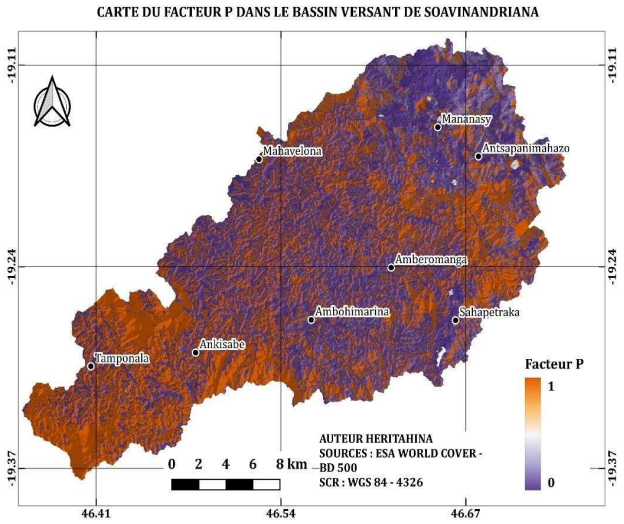

Map 7: Factor P in the Soavinandriana watershed

The analysis shows P values ranging from 0 to 1, with an average of 0.500, which we have retained for the regional level. In fact, areas where P is close to 0 are better suited to good anti-erosion practices (dense vegetation, conservation measures) than those where P is close to 1, which tend to be areas with little or no protection (and therefore more vulnerable to water erosion). This confirms intermediate conditions with low protection measures, thus justifying the adoption of P = 0.501 as the intermediate value for the regional calculation of soil loss.

IV.2.Spatio-temporal dynamics of soil erosion (A) in the Soavinandriana watershed

Map (8) below shows the spatio-temporal evolution based on the RUSLE model over a two-year period between 2016 and 2024. The spatial distribution of soil erosion (A) is expressed in tons per hectare per year (t/ha/year) in the watershed.

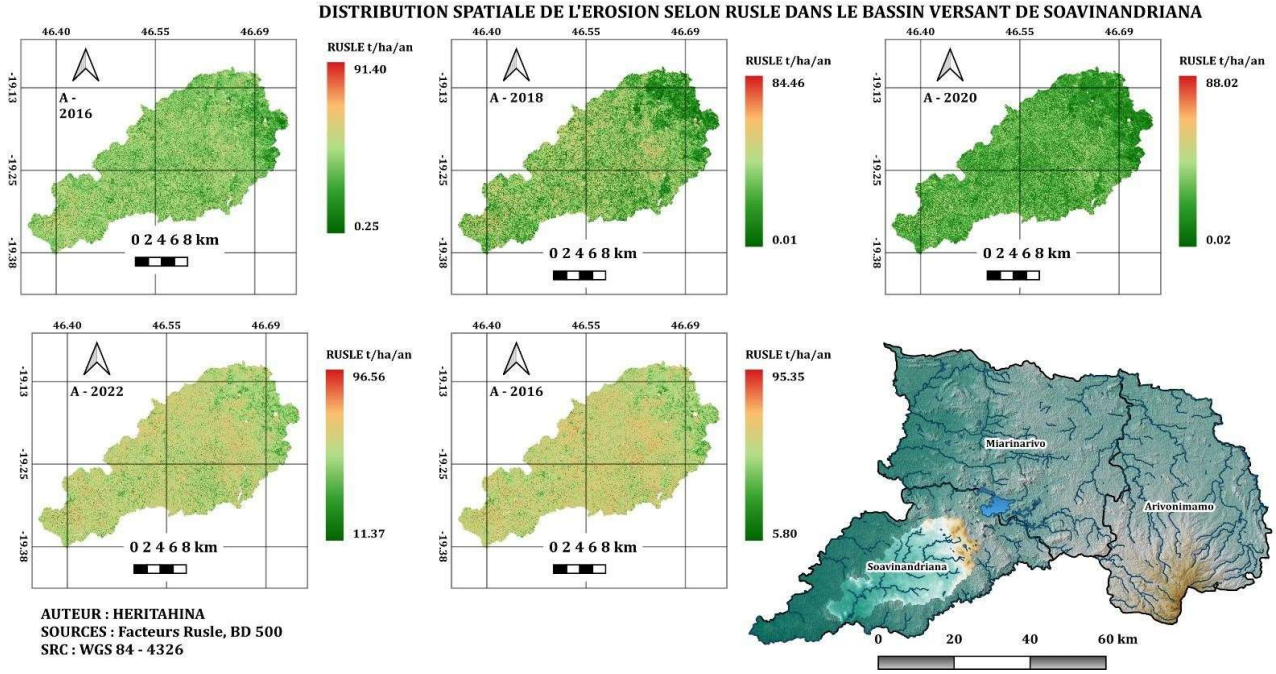

International Journal of Progressive Sciences and Technologies (IJPSAT)
ISSN: 2509-0119.

https://ijpsat.org/
Vol. 54 No. 1 December 2025, pp. 530-547

Map 8 : Spatio-temporal evolution of erosion according to the RUSLE model in the Soavinandriana watershed

The map sequence highlights a more contrasting temporal and spatial dynamic of soil loss, with erosion estimated by RUSLE remaining mostly low to moderate (often < 10 t·ha^{-1}·year^{-1}), but hotspots regularly appear on the steepest slopes and near the hydrographic network, where losses can occasionally exceed 80 to 90 t·ha^{-1}·year^{-1}. Between 2016, 2018, and 2020, the maps show a slight overall decrease in potential erosion, with large areas experiencing very low erosion. However, 2022 stands out with a marked increase in soil losses, with the minimum exceeding 10 t·ha^{-1}·year^{-1} and the maximum reaching nearly 96 t·ha^{-1}·year^{-1}, reflecting an unfavorable combination of more erosive rainfall and degradation of the protective cover. Figure (7) below summarizes the uneven spatial distribution of annual soil loss.

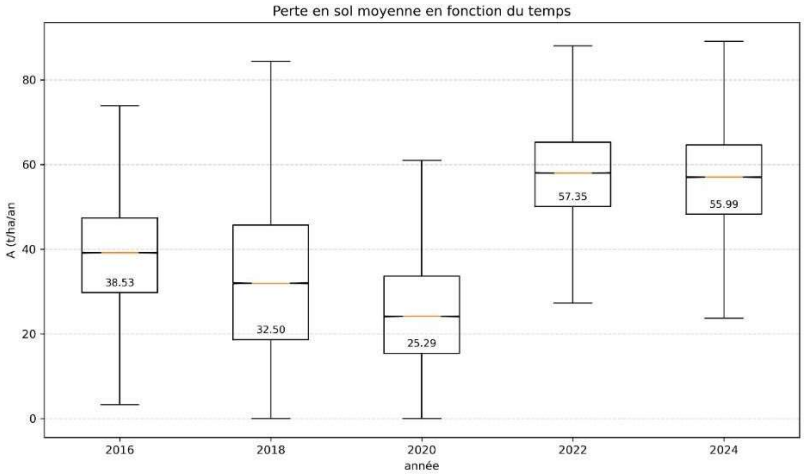

Figure 7 : Average soil loss over time

In the Soavinandriana watershed and over the entire period (2016–2024), RUSLE statistics show a clear change in soil loss. In the first part, there is a clear downward trend: average loss fell from 38.5 t·ha^{-1}·year^{-1} in 2016 to 32.5 t·ha^{-1}·year^{-1} in 2018, then to 25.3 t·ha^{-1}·year^{-1} in 2020, while the median decreased from 39.1 to 32.0 and then to 24.1 t·ha^{-1}·year^{-1}. The minimum references remain very low (close to 10^{-3} t·ha^{-1}·year^{-1}), reflecting the presence of large areas that are barely eroded. From 2022 onwards, the trend reverses: the averages reach 57.35 t·ha^{-1}·year^{-1} in 2022 and then 56 t·ha^{-1}·year^{-1} in 2024, more than double those of 2020. The maximums also increase, reaching 96.6 t·ha^{-1}·year^{-1} in 2022 and 95.4 t·ha^{-1}·year^{-1} in 2024, without this increase being accompanied by a reduction in internal variability, which remains high (standard deviations ≈ 11–13 t·ha^{-1}·year^{-1}). The box plots clearly show the shift of the entire distribution towards higher values in 2022–2024 as samples were taken during monitoring, marking the transition of the watershed from a moderate erosion regime (2016–2020) to a much higher and more widespread level of erosion in recent years.

IV.3. Quantification of soil loss in the Soavinandriana watershed

In this section, we present an analysis of soil loss in the watershed, assessing the intensity of erosion and quantifying the areas affected. The following table illustrates soil loss by erosion class between 2016 and 2024:

Table 3: Quantification of Soil Erosion by Year and Intensity Class (2016-2024)

Erosion Classes (A in t/ha/year)	2016 (ha / %)	2018 (ha / %)	2020 (ha / %)	2022 (ha / %)	2024 (ha / %)
A < 5 (very low)	5,301.86 (8.72%)	10,080.48 (16.59%)	12,969.00 (21.34%)	7,000.00 (11.53%)	9,500.03 (15.65%)

International Journal of Progressive Sciences and Technologies (IJPSAT)
ISSN: 2509-0119.

https://ijpsat.org/
Vol. 54 No. 1 December 2025, pp. 530-547

5 ≤ A < 10 (low)	12,144.81 (19.98%)	8,995.80 (14.80%)	19,712.36 (32.44%)	10,000.47 (16.47%)	14,006.69 (23.08%)
10 ≤ A < 25 (moderate)	13,444.62 (22.12%)	18,152.13 (29.87%)	14,238.16 (23.43%)	14,421.86 (23.75%)	14,874.86 (24.51%)
25 ≤ A < 50 (high)	18,505.65 (30.45%)	15,062.01 (24.78%)	10,979.99 (18.07%)	16,423.93 (27.05%)	12,213.99 (20.12%)
50 ≤ A < 100 (very high)	11,354.27 (18.68%)	8,487.42 (13.96%)	2,869.70 (4.72%)	12,866.61 (21.19%)	10,097.54 (16.64%)

To better appreciate the results, the following histogram summarizes the distribution of erosion by class according to year.

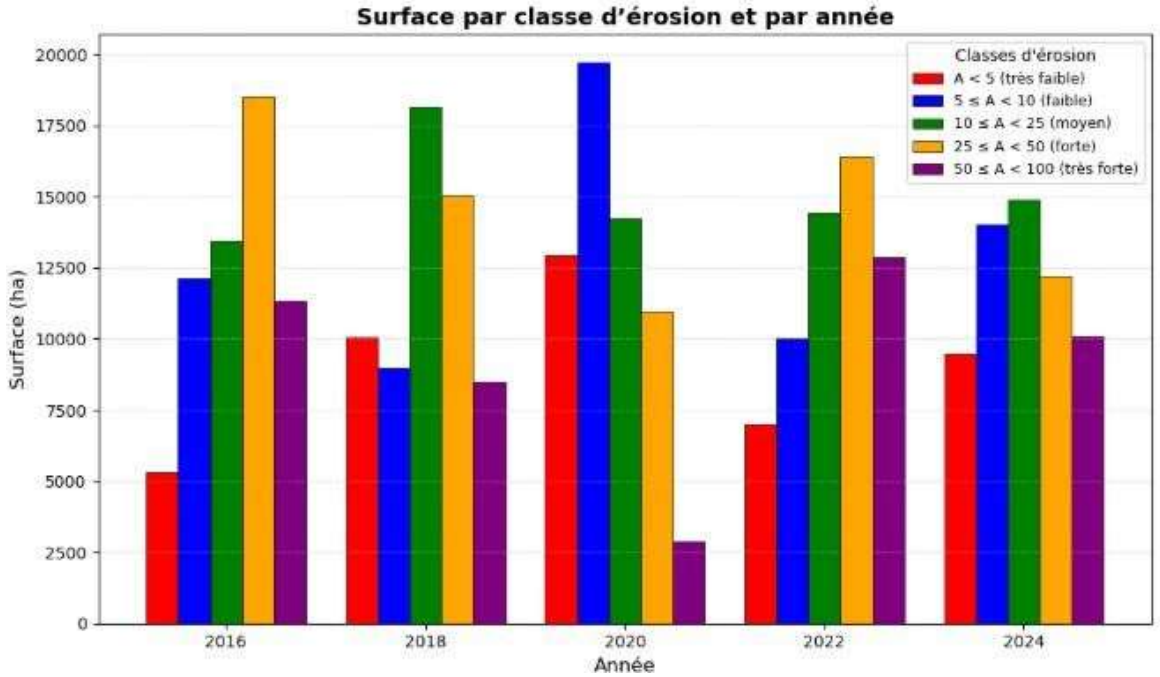

Figure 8 : Quantification of Soil Erosion by Intensity Class and Year (2016-2024)

Table 3 and Figure 7 show that in 2016 only 28.7% of the basin experienced low erosion (<10 t.ha⁻¹.year⁻¹) compared to nearly 49% experiencing high to very high erosion (≥25 t.ha⁻¹.year⁻¹), whereas in 2020 the situation improved, with 53.8% experiencing <10 t.ha⁻¹.year⁻¹ and only 22.8% experiencing ≥25 t.ha⁻¹.year⁻¹ (including 4.7% >50 t.ha⁻¹.year⁻¹); The period 2022–2024 then marks a deterioration, with areas of severe to very severe erosion rising to 48% in 2022 and then stabilizing at around 36.8% in 2024, while areas with low erosion levels represent only around 38.7%. This division into five classes highlights a structurally highly erosive context, where a significant part of the basin exceeds the erosion thresholds considered acceptable.

V. Discussions

V.1. Relationship between Factor R and A A (RUSLE) for the year 2022

Our results highlight an increase in the R factor (686 MJ.mm/ha.h.year) in 2022, reflecting the extreme rainfall recorded that year. This rainfall anomaly can be explained by a succession of major cyclonic events that hit Madagascar. Three systems in

International Journal of Progressive Sciences and Technologies (IJPSAT)
ISSN: 2509-0119.

https://ijpsat.org/
Vol. 54 No. 1 December 2025, pp. 530-547

particular contributed to this intensification: Tropical Storm Ana (January 2022), the intense cyclone Batsirai (February 2022), and cyclone Emnati (February 2022). [18] [19] . Storm Ana, at the end of January 2022, had already brought heavy rainfall to the Highlands, causing flooding in the Analamanga region. A few days later, Cyclone Batsirai crossed the country, bringing torrential rains, violent floods, and landslides as far as the central Highlands. Finally, Cyclone Emnati, on already saturated ground, exacerbated runoff and erosion in inland areas and on sloping terrain. The rapid succession of these three systems explains the exceptionally high value of the R factor during this period.

V.2. Relationship between Factor C and Factor A (RUSLE) for the year 2022

At the same time, the C factor (vegetation cover) increased significantly in the district (meaning a reduction in cover) due to widespread bush fires [20] . These events weakened the soil by reducing vegetation protection, while saturating it with water, creating ideal conditions for erosion. [21] In concrete terms, the combination of peak rainfall erosion (R) linked to cyclonic events and degraded cover (C) led to a dramatic increase in soil loss in 2022, well above the 2016–2024 average. This combination of extreme rainfall and bare soil intensifies runoff and promotes the formation of incipient gullies, as observed during the floods and landslides recorded after Batsirai and Emnati. This finding is consistent with other studies. Randriamanantena et al. (2021) applied RUSLE to the Lake Itasy basin, showing the decisive impact of rainfall and vegetation cover on erosion. Tropical environments, climatic extremes, and vegetation cover dynamics are the two main drivers of erosion variability, which is fully confirmed by our results for this watershed.

V.3. Limitations and outlook

However, the quantitative interpretation of these results must take into account certain methodological limitations. The spatial resolution of the data remains moderate: the C factor is based on NDVI series with a digital resolution of 20 m, and the 30 m ASTER DTM does not capture the micro-relief features that drive local runoff. The effective resolution of the model is often constrained by the coarsest data, particularly the R factor derived from 1 km grid climatology.

Despite these limitations, RUSLE remains a robust and widely used tool in soil conservation. It combines simplicity, reproducibility, and availability of global data, enabling large-scale applications.

VI.CONCLUSION

The spatio-temporal results of erosion in the Soavinandriana watershed show a marked change. Between 2016 and 2020, average erosion tended to decrease, but it increased sharply in 2022, before declining slightly in 2024. Our analyses show an average soil loss of around 57 t/ha/year in 2022 at the height of the crisis. At the same time, the proportion of land classified as experiencing very high erosion rose from 4.72% in 2020 to 21.19% in 2022, highlighting the severe degradation. The average RUSLE factors calculated are R = 600 to 686 $MJ \cdot mm \cdot ha^{-1} \cdot h^{-1}$, C = 0.25 to 0.5, K = 0.18, LS = 1.77, and P = 0.5, indicating a highly erosive climate combined with fragile vegetation cover. The surge in erosion in 2022 coincided with exceptionally heavy rainfall (high R index) on slopes stripped bare by slash- and-burn practices and bush fires. This combination of climatic and anthropogenic factors greatly increased the vulnerability of the soil. Previous studies confirm that such vegetation fires drastically increase erosion in tropical environments [21], and that areas with little cover (C > 0.5) suffer particularly high soil losses [22].

In view of these risks, sustainable soil management measures are necessary. We recommend in particular:

- Anti-erosion measures: planting grassy strips and hedges along contour lines to slow runoff and stabilize slopes.
- Targeted reforestation: restoration of vegetation cover on bare slopes to reduce soil loss in the long term.
- Remote sensing monitoring: regular monitoring using satellite imagery (NDVI index) and GIS to map changes in vegetation cover and erosion factors.

International Journal of Progressive Sciences and Technologies (IJPSAT)
ISSN: 2509-0119.

https://ijpsat.org/
Vol. 54 No. 1 December 2025, pp. 530-547

These recommendations aim to halt the observed soil loss. Despite a partial improvement in 2024, the persistence of heavily eroded soils in the watershed highlights the urgent need for coordinated action combining anti-erosion measures, reforestation, and scientific monitoring to preserve soil resources in the long term.

REFERENCES

[1] R. C. M. O. M. R. & A. F. M. R. N. R. G. Voarintsoa, Relation between bedrock geology, topography and lavaka distribution in Madagascar, vol. 115 (2), South African Journal of Geology, 2012.

[2] A. M. Valisoa, Sustainable tourism through heritage enhancement. Through the 4P approach (Partnership-Public-Private-Population). Case study of the Rural Commune of Mananasy, 2017.

[3] O. R. UNDP/AIED, Localization of SDGs in the Itasy region - Local consultation report, 2022.

[4] e. a. K G Renard, RUSLE Model Description and Database Sensitivity, vol. 22(3), Journal of Environmental Quality, 1993.

[5] R. N. H. et al., Modelling and Quantification of the Water Erosion of the Lake Itasy Watershed, vol. 2, International Journal of Progressive Sciences and Technologies, 2021.

[6] C. ZEBROWSKI, PROPERTIES OF THE ANDOSOLS OF ITASY AND ANKARATRA, vol. 9, O.R.S.T.O.M, 2001.

[7] D. E. D. A. L. E. À. M. RESEARCH CENTER, MONOGRAPHY OF THE ITASY REGION, 2013.

[8] L. Razafinjara, Status, priorities and needs for sustainable soil management in Madagascar, 2013.

[9] A. T. A. A. K. Adediji, Assessment of revised universal soil loss equation (RUSLE) in Katsina Area, Katsina State of Nigeria using remote sensing (RS) and geographic information system (GIS), vol. 3, Iranica Journal of Energy and Environment, 2010.

[10] C. H. Center, CHIRPS: Rainfall Estimates from Rain Gauge and Satellite Observations, Santa Barbara, CA 93106, 2025.

[11] A. E.-S. S. D. E. a. S. L. Lo, Effectiveness of EI 30 as an Erosivity Index in Hawaii, Soil Conservation Society of America, 1985, pp. 384-392.

[12] A. &. W. J. Sharpley, EPIC — Erosion/Productivity Impact Calculator, vol. Technical Bulletin No. 1768, U.S. Department of Agriculture, 1990.

[13] . &. Radziuk, oil Erodibility Factor K calculation using EPIC/USLE type models, MDPI, 2021.

[14] E. E. Pelton J., Calculating Slope Length Factor (LS) in the Revised Universal Soil Loss Equation (RUSLE), 2012.

[15] M. A. d. S. M. L. N. S. N. C. G. K. N. a. D. A. F. d. F. A. H. Oliveira, Development of Topographic Factor Modeling for Application in Soil Erosion Models in Soil Processes and Current Trends in Quality Assessment, 2013, pp. 113-138.

[16] J. J. R. &. M. L. van der Knijff, Soil Erosion Risk Assessment in Europe: A Report to the European Commission (EUR Report – Scientific and Technical Research Series), European Commission, 2000.

[17] K. F. G. W. G. M. D. &. Y. D. Renard, Predicting Soil Erosion by Water: A Guide to Conservation Planning with the Revised Universal Soil Loss Equation (RUSLE), United States Department of Agriculture, 1997.

[18] A. c. f. d. control, Tropical Storm Ana Hits hard five countries in the Southern Africa Region, 2022.

[19] GDACS, Overall Red alert Tropical Cyclone for EMNATI-22, 2022.

[20] WWF, Madagascar, a burning paradise, 2022.

[21] F. R. B. H. N. & Z. M. Akotondrabe, Dynamics of water erosion and bush fires in the Itasy region (Madagascar), vol. 2, Revue Malgache de Géographie et Environnement, 2019, pp. 45–62.

[22] G. Mohamed, Study of the impact of fires on soil erosion based on solid transport in watercourses in humid tropical environments (the Oubangui River in the Central African Republic): preliminary stage, Hydrology Laboratory, ORSTOM/Montpellier, 1996.

[23] F. K. Tobi Moriaque AKPLO, Mapping the risk of soil erosion using RUSLE, GIS, and remote sensing: a case study of the Zou watershed in central Benin | Moroccan Journal of Agricultural Sciences, Crop Production and Environment, 2020.

[24] R. C. et al., Erosion rates and sediment sources in Madagascar inferred from ^10Be analysis of lavaka, slope, and river sediment, vol. 4, The Journal of Geology, 2009.